UCRL-17094-Rev.

University of California

Ernest O. Lawrence Radiation Laboratory

EFFECT OF INITIAL DISLOCATION DENSITY ON THE STRESS STRAIN CURVE AND ON SURFACE INDICATION OF SLIP IN COPPER

DISCLAIMER

Canadian J. of Phys.

UCRL-17094-Rev.

UNIVERSITY OF CALIFORNIA
Lawrence Radiation Laboratory
Berkeley, California

AEC Contract No. W-7405-eng-48

EFFECT OF INITIAL DISLOCATION DENSITY ON THE STRESS STRAIN CURVE AND ON SURFACE INDICATION OF SLIP IN COPPER

J. Washburn and G. Murty

September 1966

EFFECT OF INITIAL DISLOCATION DENSITY ON THE STRESS STRAIN CURVE AND ON SURFACE INDICATION OF SLIP IN COPPER

J. Washburn and G. Murty

Inorganic Materials Research Division, Lawrence Radiation Laboratory,
Department of Mineral Technology, College of Engineering
University of California, Berkeley, California

INTRODUCTION

The clearly non uniform distribution of slip as revealed by surface slip markings is one of the earliest experimental observations regarding the nature of plastic strain in crystalline materials.[1] Yet it is a feature of plastic deformation that is still not adequately explained by existing theories of yielding and strain hardening. Surprisingly, there is even a need for more accurate experimental information on the way in which successive shear displacements are distributed during each increment of plastic deformation. The details of slip band growth and the shape of the stress strain curve vary with temperature of deformation, dislocation density, stacking fault energy and the ratio of resolved shear stress on primary compared to secondary slip systems.[2,3] The authors are unaware of any systematic experiments using electron microscope replica techniques in which the same surface area has been observed repeatedly after several small increments of strain so as to follow the growth of slip bands under a variety of conditions. The most extensive previous experiments on the slip band structure in copper are those reported by Mader.[4,5] Active slip bands were studied by electropolishing the surface of tensile specimens after reaching various points on the stress strain curve. Electron microscope replicas were then taken after additional 5% increments of strain. In this way only the last formed

slip markings were observed. He showed that during stage I in a specimen, loaded so as to produce single slip, the individual shear displacements were small and a very large number of planes were active during a 5% strain increment. Most slip markings were very long, many extending entirely across the specimen. In stage II, during rapid strain hardening, the shear displacements became more localized into fewer more prominent bands. The average displacement per slip band was estimated to be about 25 b. Prominent slip bands were found to have been fully formed within a strain increment smaller than 5% and did not generally grow longer if a 10% strain increment was given. The average length of prominent newly formed slip bands decreased linearly with strain measured from the beginning of rapid hardening (stage II). As the crystal was deformed into stage III active slip bands became wider and still fewer in number and they were often observed to be linked together by short slip bands on the cross slip system.

In the present set of experiments more extensive observations on slip bands in copper have been made by repeatedly observing the same area after several small increments of strain and by observing the same areas at both electron microscopes and optical magnifications. In addition the effect of initial dislocation density on the three stages of the stress strain curve and on the growth of slip bands was studied. It was hoped that the experiments would provide new information that would be helpful in arriving at correct explanations for the three stages of the stress strain curve and contribute to a better understanding of strain hardening.

EXPERIMENTAL PROCEDURE

Preparation of Test Specimens:

High purity copper (99.999%) was obtained from American Smelting and Refining Company. Seeded large single crystals (1× 4 ×15 cm) were grown from the melt in vacuum using graphite crucibles. The geometry of the specimens is shown in Fig. 1a. The crystal faces were parallel to $(1\bar{2}1)$ and $(\bar{1}01)$. The long axis was parallel to [111] within about 3°.

In order to obtain high initial dislocation densities in some specimens, several of these large crystals were prestrained. The first was subjected to an explosive shock pulse at a pressure of 10 kbar. This shock load was weak enough so that no twins were formed except near one end. Shock loading was expected to cause multiplication on all 12 slip systems. To avoid the possibility of twinning, the other large crystals were prestrained by tensile elongation along the $\langle 111 \rangle$ multiple slip axis. Polycrystalline OFHC copper blocks (1.2× 5 ×6.5 cm) were joined on either end of the long dimension of the crystal, by electron beam welding. The polycrystalline blocks acted as grip sections. The resolved shear stress that was reched during prestraining varied from 0.73 kG/mm^2 to 6.70 kG/mm^2.

Smaller crystals of easy glide orientation were cut from both annealed and prestrained large crystals at 45° to [111] and $[\bar{1}01]$ axes with an acid saw. In the case of the shock loaded crystal specimens were taken from the twin free regions. The cut surfaces of the crystal samples were polished with an acid polishing wheel. The dimensions of the easy glide orientation samples, after acid sawing and polishing, were about 1.5× 8 ×50 mm. They were then electropolished using a

solution of 25% phosphoric acid, 25% ethyl alcohol and 50% distilled water at about 10°C.

The geometry of the test specimens is shown in Fig. 1b. The (111) plane that was inactive during prestraining, was the primary glide plane for the crystals of orientation "B". In these crystals, the trace of the glide plane on the top (8×50 mm) surface was normal to the tensile axis and the primary Burgers vector was at 45° to the normal of the top surface.

The crystals were deformed in an Instron testing machine at a strain rate of 6.6×10^{-5}/sec. The gauge length was 25 mm. A special fixture was used during mounting and removal from the Instron testing machine to avoid bending of the crystals. The shear stress - shear strain curves were computed using the usual formulae for single glide assuming lattice rotation to result from glide on the primary system only.

Observation of slip markings:

During stage I the tensile test was repeatedly interrupted for surface observations. One or two percent shear strain increments were used. The surface contour of the crystals at the end of each strain increment was studied using selected area optical and electron microscope replica techniques. In order to show whether deformation took place primarily by the formation of new slip lines or by the growth of the already existing slip lines, surface observations were repeated at the same spot of the crystal without intermediate polishing for several consecutive strain increments. Macroscopic distribution of slip was also followed by observing the whole gauge length of the crystals at very low magnification.

Similar observations to those made during stage I were made throughout the linear hardening region (stage II). The crystals were polished at the beginning of stage II in order to study the slip lines that are formed in stage II without the background of slip markings already formed in stage I. Shear strain increments of 5-10% were used in order to compare results with previous work.[4] At three different strains within stage II "active" slip line observations were made by polishing and then observing the surfaces after 2% and 4% strain increments.

The annealed crystals were polished at the beginning of stage III of the stress-strain curve and observations were made after 2-10% strain increments.

In order to make a series of observations on the same area of the specimen, it was necessary not to destroy the surface after each replication. A two-stage formvar-carbon replica technique was used.[6] The final replica was directly mounted on the supporting ring of the specimen holder of a Hitachi Electron Microscope without using any grid. Thus the specimen carrier was a brass ring (outside diameter 3.5 mm) with an orifice of 0.38 mm diameter at the center. Large areas (about $10^4 \mu^2$) on the final replica could be viewed without the obstruction of grid bars.

In order to make successive replicas of the same area of the crystal, the following procedure was used. A rectangular zone of 2.0 × 2.5 mm was marked on the crystal surface by drawing fine scratches with the diamond indentor of a microhardness tester. The longer dimension of the zone was perpendicular to the crystal axis. Two microindentations of the smallest possible dimensions were made in the center of the rectangular zone. The two microindentations were 0.38 mm apart. They were located

on a line perpendicular to the crystal axis. These microindentations were used as reference marks on the final replica. The primary replica was shadowed with tungsten oxide from a "V" shaped filament. The yellow tungsten oxide was first obtained by heating a tungsten filament in air.

Observations of the replicas were made using a Hitachi (HU-11A) electron microscope operated at 50 kV. Large areas ($40 \times 30\mu$) of the central portion of the replicas were photographed. Positions of the specimen that had been selected on the crystal with the light microscope could thus be identified again on the replicas. In this way, the electron micrographs of a specific surface region of a crystal after several strain increments could be obtained along with the corresponding optical micrographs. Comparisons among electron micrographs of the same area with different strain increments and with the optical pictures of the same surface region were possible.

Repeated optical observations on the same surface region of the crystal after several strain increments were made using Zeiss and Leitz metallographic microscopes. Optical observations were made with either oblique or dark field illumination. In order to avoid grip effects at each end of the crystals, slip line observations were always made on the central portion of the gauge length of the specimens.

In some cases shear displacements for individual slip bands were measured directly using the latex ball method.

RESULTS

Stress-Strain Curves:

Stress-strain curves for typical annealed and prestrained crystals are shown in Fig. 2. All the curves were characterized by three stages.

The initial yield stress of the crystals that were not prestrained was about 150 gm/mm^2. This value is somewhat higher than that usually obtained for annealed copper crystals of comparable purity. In these experiments, the copper crystals were grown in hard graphite molds from seed crystals; they had a relatively high dislocation density ($\sim 10^7$). For the prestrained specimens the direction of the tensile axis was changed from a multiple slip orientation during the prestrain to an easy glide orientation. The initial flow stress on the new primary slip system was always higher than the highest resolved shear stress reached during the prestrain. The ratio of the initial resolved shear stress on the new slip system to that reached during prestraining was about 1.25 - 1.35. The strain hardening rate was always initially small. The initial hardening rate decreased and the length of the stage of low hardening rate increased with increasing prestrain. The specimen that was prestrained to 6.70 kG/mm^2 in mulitple slip orientation, necked and fractured by shear without any general elongation in the easy glide orientation. Parameters taken from the stress-strain curves are shown in Table I.

In addition to the important effect on the initial portion of the stress-strain curve, the previous strain history strongly affected the strain hardening rate and the extent of the second linear hardening stage. The hardening rate decreased and the length increased with increasing prestrain. The stress level τ_{III} at which the hardening

Table I. Parameters of the Stress-Strain Curves

	No prestrain	Prestrained by shock loading (10 kbar)	Prestrained to 2.54 kG/mm^2
Stage I (Easy Glide)			
Shear Strain at the End of Stage I (ϵ_{II})	0.05	0.12	0.17
θ_I/G	5.0×10^{-4}	2.5×10^{-4}	4.0×10^{-5}
Stage II (Linear Hardening)			
Extent of Stage II ($\epsilon_{III}-\epsilon_{II}$)	0.22	0.36	0.40
$K = G/\theta_{II}$	400	890	1730
Shear Stress at the End of Stage II (kG/mm^2) (τ_{III})	2.4	3.6	4.1

rate began to decrease was found to increase from 2.4 kG/mm^2 to 4.1 kG/mm^2 with increasing prestrain. Three stages were typical of the stress-strain curves of all prestrained specimens, even when the inital flow stress level was higher than τ_{III} at which stage III begins for the as grown crystal. At very large strains all the stress-strain curves approached the same saturation stress level.

Surface Observations on As-Grown Crystals:

(Stage I)

During stage I slip distribution was non uniform along the gauge length of the crystal. Figure 3 shows an appreciable portion of the gauge length after three successive strain increments. After 1% shear strain, there were regions on the crystal surface with a high density of slip markings separated by others where no visible slip had appeared. Individual slip markings were propagating from one edge of the crystal to the other. With increasing strain, the undeformed regions of the crystal became filled with slip markings. By the end of stage I, the closely spaced slip offsets had a wavy appearance when viewed at very low magnification (Fig. 3c).

At higher magnification the surface contour had an entirely different appearance. The same area on the crystal surface is shown in Figs. 4a,b, and c after 1, 3 and 5% shear strain respectively. On this scale shear strain appeared to be distributed more uniformly. Individual faint slip lines appeared early in stage I that continued to grow with increasing strain becoming more and more prominent. New faint lines also formed throughout stage I. The lengths of individual slip markings could best be estimated at intermediate magnification in dark field (Fig. 5). The average length was about 220μ and did not

change with increasing strain increment during this stage. No direct measurement of the step heights of slip markings was possible due to their fine nature. Typically the shear displacement was maximum at the center and decreased very gradually toward both ends making the estimate of length somewhat arbitrary.

(Stage II)

Slip markings formed in stage II were also fine. In general, they became shorter and stronger than those formed during stage I. No regions were free from new slip markings along the gauge length for a 1% strain increment, but regions of different slip band density were observed (Fig. 6). Slip bands often seemed to form correlated groups; one beginning near where another ended. These can be clearly seen in Fig. 6. Many new slip bands appeared and the continuous growth of slip bands was less frequent than in stage I. The fine structure is shown in Fig. 7. The same area on the crystal surface is shown after 5 and 15% shear strain increments in stage II. Growth of some of the bands present after 5% strain in stage II during the subsequent 10% increment can be clearly seen. There was a very great dispersion in the contrast of individual slip lines, even towards the end of stage II. The shear displacement for the most prominent bands as estimated by the latex ball method was about 100 b. Therefore the number of dislocations that had emerged at individual bands ranged over at least one order of magnitude.

Active slip band observations in stage II were carried out at 7, 15 and 23% total shear strain. Shear strain increments of 2 and 4% after polishing were used for this purpose (Fig. 8). Active slip bands formed near the end of stage II were shorter than those formed near

the beginning and their lengths did not change during the additional strain increment of 2%. Slip markings on the side surface (parallel to the primary Burgers vector) were always approximately two times longer than those on the top surface. The average length of active slip lines decreased linearly with increasing strain.

Surface Observations on Explosively Prestrained Crystals:

The initial flow stress of these crystals was about 1.8 kG/mm^2. During the first low hardening stage for these specimens the distribution of strain along the gauge length was much more clearly inhomogeneous than was the case for as grown specimens.

One or more Luders bands propagated in several widely separated regions along the gauge length. However, no yield drop at the beginning of plastic flow or fluctuations in the load during the region of small hardening rate were observed. Figure 9 shows the Luders band front as it passes through a particular field of view. The left end of these micrographs corresponds to an edge of the crystal. Groups of slip bands were always observed to nucleate at this edge and then propagate across the width of the crystal by formation of new bands near the end of the previously formed band. This type of slip band propagation continued until the whole gauge length of the crystal was uniformly filled. The end of the region of small hardening rate clearly coincided with the filling up of the gauge length with slip bands.

The slip bands could be resolved into clusters of fine slip on the replicas. Figure 10a, b, and c show electron micrographs of the same spot on the crystal surface and the corresponding optical micrographs after successive strain increments. More and more fine slip lines were added at the sides of the bands, but it was not possible to

see whether additional shear was taking place on already existing fine lines as the strain increased. Also, it was not possible to count the number of fine lines within each wide band. For the most prominent shear markings seen on the replicas offsets were measured to be of the order of 150 Burgers vectors. The fine structure within a typical slip band near the end of the region of small hardening rate is shown in Fig. 11.

Slip bands continued to form and grow during the linear hardening (stage II) part of the stress strain curve in much the same way as in stage I except that they were distributed more evenly along the gauge length (Fig. 12). Correlated groups of slip bands were a prominent feature of the strain distribution as was the case for as grown crystals. At high magnification the bands seen optically could be resolved as clustered fine slip (Fig. 13). Active slip band observations were made at 16, 26, and 36% total strain. For 2% strain increments the average length of individual bands, as observed in dark field, decreased linearly with increasing strain from about 4×10^{-3} cm to 2×10^{-3} cm (Fig. 14).

Surface Observations on Heavily Prestrained Crystals:

For these specimens, the resolved shear stress reached during prestraining in multiple slip was 2.54 kG/mm^2 and the shear stress at which plastic flow started on the new slip system was 3.25 kG/mm^2. In the low hardening rate region (stage I) the slip distribution was similar to that for more lightly prestrained specimens just decribed except that the non-uniform distribution of slip bands and clustering of fine slip became even more pronounced. The slip bands were narrower. They again initiated at one edge of the crystal and propagated to the opposite edge (Fig. 15). In these specimens alip bands were linked

together by prominent cross slip.

The fine structure of the sharp slip bands could not be well resolved even on the replicas (Fig. 16). The width of and the local shear strain within individual bands increased continuously to 1/2μ and 0.7 respectively by the end of the first stage.

During the linear hardening stage bands again developed as in stage I except that new bands gradually became more uniformly distributed along the gauge length. Pre-existing bands continued to grow and new ones were formed. The correlation between newly forming bands was even more marked in this specimen (Fig. 17). The average length of newly formed or "active" slip bands again decreased linearly with strain as observed on optical dark field micrographs (Fig. 18). Figure 19 summarizes the observations on active slip band lengths for stage II for specimens of the three different initial dislocation densities.

DISCUSSION

Nucleation of Slip: For prestrained specimens, new waves of slip clearly started by formation of a large enough group of primary dislocations near the edges of the rectangular specimen. The formation of this first slip band promoted the growth of others in the region of stress concentration around its front. Therefore, once the first slip band was formed, slip propagated right across the specimen, not as a single slip band, but as a correlated group of slip bands. This mode of deformation was less obvious in specimens that had not been prestrained but, as shown by Fig. 6, it still was present. The flow stress under these conditions should be the stress at which in regions of stress concentration primary dislocation loops can multiply so as to produce a large enough slip band to set off the avalanche of slip.

Occasionally classical Frank Read sources may provide the necessary group of primary loops. However, considering the nature of dislocation tangles in deformed crystals or even the network of dislocations in an annealed crystal, this should rarely be possible.

The longest dislocation segments that can potentially act as Frank Read sources should seldom be isolated enough from other dislocations so that a source can develop according to the classical picture. New attractive junctions with intersecting forest dislocations would usually be formed before the first cycle of operation can be completed. If the original segment was longer than the average network length, this is almost certain to occur.

It seems likely that the generation of a group of like dislocations on the same or close-by glide layers, which constitutes the nucleation

of a slip band, usually involves cooperative motions of many dislocation segments rather than classical source operation.

When a small stress is applied to an annealed crystal, the first segments to glide should be those sustaining the highest resolved shear stress that lie on a {111} plane. If the stress is less than $\frac{\mu b}{\ell}$, where ℓ is the average length of dislocation segments in the three dimensional network, μ is the elastic shear modulus and b is the Burgers vector, then the distance moved will generally be small. Motion terminates when the bowing dislocation reaches the equilibrium radius of curvature corresponding to the applied stress. If the bowing segment is initially longer than the average for the network, even if it is longer than the critical Frank Read length $\frac{\mu b}{\tau}$, it will usually come up against other dislocation segments that pierce its glide plane before it reaches equilibrium curvature. By forming new attractive junctions with some of these intersecting dislocations its length will be reduced to something close to the average length for the network. The mechanism of slip band nucleation proposed here is based on the idea that bowing of a highly mobile segment on the primary glide system will sometimes promote cooperative glide of several connecting forest segments that will in turn allow the bowing segment to continue to expand even though the applied stress is less than $\frac{\mu b}{\ell}$.

When a dislocation loop, expanding on the primary glide plane, is held up by strong elastic interactions with intersecting dislocations, some of the intersecting dislocations may be caused to move on their

own glide surfaces, allowing a further advance of the primary dislocation. This should frequently occur at a stress smaller than that necessary to complete the intersection (i.e. to cut the intersecting dislocation). The direction in which a pinning point due to an intersecting dislocation can move, without involving nonconservative motions of the dislocations involved, depends on the Burgers vector of the intersecting dislocation. For the FCC structure, if the Burgers vector of the forest dislocation is one of the three that lie in the primary glide plane, then the trace on that plane of all its possible glide surfaces is a straight line parallel to the Burgers vector and passing through its initial position. If the intersecting dislocation has a Burgers vector that does not lie in the primary glide plane, then the trace of its glide surface on the primary plane can follow any path.

If forest dislocations are caused to glide, the distance between pinning points for some segments of the bowing primary dislocation increase as illustrated by Fig. 20. The longest bowing segments may grow slowly by this process to the length $\mu b/\tau$, where τ is the resolved shear stress in the primary system. In this way the primary dislocation can continue to move forward, successively pushing aside the most easily displaced intersecting dislocations. The moving dislocation loop would follow a tortuous path partially clearing away the forest of intersecting dislocations in the neighborhood of its glide plane as shown in Fig. 21.

The stress at which cooperative rearrangements of a network can take place should be controlled by the dislocation density and the mobility of the segments that do not lie on {111}. According to this picture,

nucleation of a slip band would involve cooperative bowing of a part of the network having dimensions larger than the average length of individual segments.

Slip bands would be formed at the critical stress necessary to cause some bowing segments to start to clear parts of the forest. The partially cleared areas that would be created should often turn back on themselves as in Fig. 21b. Wherever this happened a dipole would be formed because the sum of the components of the Burgers vector of the intersecting dislocations in the encircled part of the forest would not generally be zero. The cleared area might occasionally reach the back side of the original starting point, as in Fig. 21c, or turn back on itself, as in Fig. 21b, at a point where a segment of the expanding loop has been annihilated by recombination with a forest dislocation of antiparallel Burgers vector. When this happens a slip band source will have been nucleated. The dislocation loop can then repeatedly follow the already cleared path. Each successive trip around the circuit would generally be on a glide layer displaced above or below that of the immediately preceding passage for the same reason as that pointed out above in connection with dipole formation. The pile-ups of dislocations of the primary system that will form against the boudaries of the cleared areas would usually consist of dislocations of like sign on a set of equally spaced levels.

As the cleared areas expand, pile ups of opposite sign will tend to get pushed together to form the dipole braids that are observed in stage I by transmission electron microscopy.[7]

Clustering of Fine Slip: In copper the slip bands that are seen by the optical microscope are always the result of small shear displacements on a great many glide layers rather than large displacements on a few. Generation of one or a few primary dislocation loops on a given glide layer, perhaps by the cooperative bowing mechanism just descirbed, seems to promote similar multiplication on other glide layers near the first. This tendency for slip bands to rapidly widen may be explained by considering another effect that primary dislocation loops can have on the forest of intersecting dislocations: The expansion of a few loops of primary dislocation on a given glide layer may promote multiplication of primary loops on near-by layers by partial annihilation of the forest tangles, within a zone above and below the original glide layer.

It is suggested here that dislocation tangles are usually only metastable and may become unstable in the presence of primary dislocations. The forest will generally contain dislocations of all six Burgers vectors that are arranged in an irregular network that has reached a condition of metastable equilibrium with respect to conservative motions. However, each segment will be split into partials on one or the other of its two possible {111} glide planes. Futher rearrangements and concomitant decrease in dislocation density would usually take place if all segments were free to change glide planes. It is because they are split into partials that this is not the case. Most dislocation tangles in a deformed crystal separate neighboring subgrains that are only slightly misoriented relative to one another. The total length of dislocation line present is usually far greater than that which is

necessary to account for the tilt or twist angle between the two subgrains. Therefore, there are many pairs of opposite sign that are prevented from gliding together to annihilate because they are in positions of metastable equilibrium.

The passage of a group of primary dislocations into such a dislocation tangle should generally cause further rearrangement and promote annihilation. This should be particularly true when the tangles have been formed and reached metastable equilibrium under a different applied stress as is the case for tests in which the active slip system or systems are changed.[8] However, even when a crystal is strained from the start in a single slip orientation, multiplication of dislocations on secondary systems and across slip of primary dislocations produces dislocation tangles that generally contain almost equal lengths of dislocations of all Burgers vectors.[7] Therefore, it seems likely that growth of a slip band can in all cases be aided by the inherent instability of the dislocation tangles within which the net Burgers vector is often almost zero.

The interactions that would lead to local annihilation would usually be complex, but two rather idealized examples are given for screw dislocations (Fig. 22) and edge dislocations (Fig. 23).[9] A small section of a dislocation tangle is shown in Fig. 22 in which four $\frac{1}{2}[10\bar{1}]$ screw dislocations on the $(1\bar{1}1)$ slip plane have interacted with two intersecting dislocations that lie in $(\bar{1}11)$. The plane of the drawing is (101) or any other plane in the $[10\bar{1}]$ zone. The $\frac{1}{2}[10\bar{1}]$ dislocations of one sign form attractive junctions with the intersecting dislocations while those of the opposite sign are repelled. However,

the latter are attracted by the former and will, therefore, be held against the intersecting dislocations. An element of dislocation tangle like that shown in Fig. 22 will become unstable if dislocations of the same Burgers vector are introduced that are split on (111) instead of on $(1\bar{1}1)$. Therefore, multiplication of dislocations on (111) would result in annihilation of this metastable arrangement of screw dislocations.

An edge dislocation in a tangle is frequently stabilized by being close to another edge dislocation of opposite sign that lies on a different glide plane. As a simple example suppose that a jogged screw dislocation has moved leaving behind two dipoles; a section through the two dipoles in represented by Fig. 23a. The dislocations A and B lie on the same glide plane, they are of opposite sign and would glide together and annihilate except that they are stabilized by dislocations A' and B'. If it is assumed that these two dipoles have the same Burgers vector as the primary system, and if $\frac{D}{d} < \frac{d}{b}$ where D is the distance between dipoles and d is the spacing between dislocations in the dipoles, then A and B can be annihilated by intersection cross slip as shown in the sequence of Fig. 23 (b,c). In this way some dislocations of the intersecting forest will be destroyed. In both these examples, the network dislocations that would be annihilated have the same Burgers vector as the primary system. However, even where the active slip system has not been changed, many such dislocations should be expected to be present with the tangles because each attractive intersection tends to promote cross-slip. Hirsch first

pointed out that a dislocation that intersects a pile-up on its cross-slip plane would be pulled into the cross slip plane.[10] Figure 24 shows how this may happen even at isolated attractive intersections.[11]

Assume that a moving dislocation $\frac{1}{2}[1\bar{1}0]$ on (111) intersects a forest dislocation $\frac{1}{2}[011]$ which lies on $(11\bar{1})$. A segment of the resultant $\frac{1}{2}[\bar{1}0\bar{1}]$ will be formed along the $[1\bar{1}0]$ line of intersection of the two planes. If the moving dislocation in the figure has been traveling from front right to back left, then as it starts to bow out on either side of the junction, the segment at the left adjacent to the contracted node will necessarily pass through the pure screw orientation. For the opposite direction of motion it would be instead the segment at the right adjacent to the extended node. In either case for an instant the three dislocations, $\frac{1}{2}[1\bar{1}0]$, $\frac{1}{2}[011]$, and $\frac{1}{2}[\bar{1}0\bar{1}]$ where they meet must all lie in their common $(11\bar{1})$ glide plane which is also the cross slip plane for the moving dislocation. To establish equilibrium of line tensions the node will tend to move into the cross slip plane as shown in Fig. 24b. For undissociated dislocations there is nothing to prevent this rearrangement. When the $\frac{1}{2}[1\bar{1}0]$ dislocation is split into partials in (111) and it is the contracted node that tends to move into the cross slip plane, a second constriction must be formed and moved away from the node as the latter leaves the line of intersection. However, for a case like the one illustrated by Fig. 24 the energy gained from shortening of the total length of dislocation line would be greater than that associated with a constriction. When it is the extended node that tends to move into the cross slip plane the constriction that is already present simply

has to slide along the line of intersection as the node moves away from it. Therefore, thermal activation should frequently not be necessary even for split dislocations.

What happens after the stage shown at Fig. 24b depends largely on what occurs at the other extremities of the dislocation lines (those not shown in the figure). For example, if B moves forward more rapidly than A then segment 00' will shrink and 00" will be annihilated as part of segment 0B folds back upon it. The moving dislocation will have completed its cutting of, CD. However, if A continues to move while B remains stuck at another intersection and if there is a large enough component of stress acting in the cross slip plane the node may continue to slide up the intersecting forest segment as the constriction moves away along $[1\bar{1}0]$. The $\frac{1}{2}[\bar{1}0\bar{1}]$ segment, 00', is elongated as an increasing length of the moving dislocation glides into the cross slip plane. This segment, 00", of $\frac{1}{2}[110]$ dislocation may then develop as a source for slip in the cross slip plane.

Another type of intersection that would facilitate "cross slip" is the cutting of a segment of dislocation having the same Burgers vector as that of the moving dislocation but lying in the cross slip plane. This dislocation segment might not have been able to move prior to the intersection because its length would be less than the critical Frank Read length for the local resolved cross slip stress. The intersection would produce a geometric situation similar to that pictured in Fig. 24 except that there would be no connecting junction dislocation. A length of the moving dislocation would be drawn into the cross slip plane, again as a result of line tension. As was the

case for the extended node, in the previous example, no second constriction would be needed.

The annihilation of segments of the same Burgers vector within near by parts of the dislocation tangles would certainly promote further rearrangements that would result in shortening the total length of dislocations of other Burgers vectors. This, in itself, might be enough to explain the growth of slip bands. However, it is probable that a group of primary dislocations represents a sufficient stress concentration so that multiplication of dislocations of the other two coplanar Burgers vectors will always be associated with its motion. There is strong experimental evidence that other slip systems in the primary plane do act together with the primary system. Slip markings are visible on polished surfaces that contain the primary Burgers vector direction.[33] If this is the case then annihilation like the examples of Figs. 22 and 23 would occur for three of the six Burgers vectors rather than for just one of them.

The Strain Hardening Rate: Stage I: Usually a sharp distinction has been made between progressive spreading of slip along the length of a specimen (Luders band deformation) and the "easy glide" deformation that occurs in stage I when crystals in single slip orientation are extended in tension. It is the opinion of the present authors that no sharp distinction can be made. Specimens that have been prestrained under different deformation conditions, either by explosive shock loading or <111> extension very definitely deformed in a progressive manner during the first stage of the stress strain curve. However, it is not

equally clear that the first stage for annealed specimens was not progressive. Low magnification observations even suggested that it was. The presence of a finite hardening rate has sometimes been used as a criterion that a deformation is not of the Luders band type. However, for Luders band deformation the hardening rate is simply an indication of the uniformity of the initial defect substructure and stress distribution. If the specimen is completely homogeneous, then the slope of the stress strain curve will be zero. If it is not, there will be a finite slope. For an annealed crystal, subgrain boundaries and slip that occurs on secondary systems during pre-yield deformation are almost unavoidable causes of inhomogeniety. The finite slope that is always obtained for stage I may simply reflect this inhomogeniety. For the prestrained specimens it was clear that during the first stage the dislocation substructure that was produced during the prestrain was gradually being replaced by one that had greater stability under the new deformation conditions. However, as the amount of prestrain is reduced the stress strain curve and the surface slip markings changed gradually to those typical of an annealed crystal. This suggests that even in the annealed crystal the grown-in dislocation substructure, with the changes in it that have occured during pre-yield deformation, should be considered as an unstable dislocation arrangement that is gradually replaced by a more stable one during stage I. According to this picture, stage I ends when the original dislocation arrangement has bee replaced in all parts of the volume. Only for the case where the resolved shear stress on the next most favored slip plane is initially appreciably less than

that on the primary system does this replacement require a large strain. When more than one slip plane becomes active simultaneously a relatively stable three dimensional cell structure develops very quickly. The dipoles and dislocations left along the active glide layers of one system act as barriers to the intersecting system and visa versa. The dislocation density increase associated with a given increment of strain is thus dramatically increased. Even for the single slip orientation, a second slip plane may become active if resolved shear stress on it becomes equal to the yield stress at which extensive slip originally began on the primary system. In this case stage I is rapidly terminated.

Stage II: The results of slip line observations on prestrained specimens show that there can be no general correlation between strain hardening rate and slip line parameters. Strain increments which result in identical slip markings can come from a region of rapid hardening in one specimen and a region of no hardening in the other. This is the case if one compares the "active" or newly formed slip markings in the initial horizontal part of the stress strain curve in a lightly prestrained specimen with those formed at the same stress level during rapid hardening of an annealed crystal. Furthermore, the meaning of measured slip line parameters is questionable. Slip line lengths and spacings tend to be rather subjective measurements because they depend so strongly on the degree of prominence which is recognized as a slip band for the purpose of the measurements. There is another serious difficulty in the interpretation of slip band lengths.

Slip bands are often closely correlated with each other. This was very clearly the case for prestrained specimens. As shwon in Figs. 12 and 17, a slip band nucleated at one edge of the specimen then new bands formed along the slip front in much the same manner that a crack might propogate through a crystal. This process continued until the wave of slip had passed entirely across the crystal. There may have been almost complete relaxation by local rearrangements within the dislocation tangles at the regions where the shear displacement shifted from one set of levels to another. If this is the case, then the apparent slip band lengths have little significance. This relaxation can certainly occur without prominent cross-slip markings if there is considerable overlapping of the two adjacent slip bands. This was often the case; one band gradually becoming less prominent while the other gradually took over on the new level.

All specimens, even the heavily prestrained ones, exhibited three stages, on the stress strain curve. This was true even when the yield was at a level that in an annealed crystal, tested at the same temeprature and strain rate would have been in stage III. This shows that even in a specimen in which slip bands are always obviously linked together and always form a correlated group that starts at one corner and grows entirely across the specimen, the stress strain curve for the single slip orientation still has the same general shape. The most frequently accepted explanations for the three stages cannot explain this behavior.

The results of this investigation suggest that no general theory of strain hardening can be successful if it is based only or even primarily

on the arrangement of dislocations left in the crystal as seen by transmission electron microscopy; the sample observed is too small. The macroscopic and microscopic distribution of shear strain along the length of the specimen are extremely important in determining the shape of the stress strain curve.

ACKNOWLEDGEMENTS

This work was done with the financial support of the United States Atomic Energy Commission through the Inorganic Materials Research Division of the Lawrence Radiation Laboratory.

REFERENCES

1. O. Mügge, Gotting. Nachr. (1899), 56.

2. L. M. Clarebrough and M. E. Hargreaves, Prog. in Metal Physics, 8, 1 (1959).

3. R. W. K. Honeycombe, Progr. Mater. Sci. 9, 95 (1961).

4. S. Mader, Z. Physik, 149, 73 (1957).

5. S. Mader, Electron Microscopy and Strength of Crystals (Interscience Publishing Company, New York, 1963) p. 183.

6. J. T. Fourie, J. Appl. Phys. 29, 608 (1958).

7. U. Essmann and H. Kronmuller, Acta Met. 11, 611 (1963).

8. Z. S. Basinski and P. J. Jackson, Phys. Stat. Sol. 9, 805 (1965).

9. J. Washburn and G. Murty, J. Appl. Phys. 37, 2511 (1966).

10. M. J. Whelan, P. B. Hirsch, R. W. Horne, W. Bollman, Proc. Roy. Soc. A, 240, 524 (1957).

11. J. Washburn, Appl. Phys. Letters 7, 183 (1965).

FIGURE CAPTIONS

Fig. 1 Geometry of the crystals showing how specimens of easy-glide orientation B were cut from large crystals of orientation A.

Fig. 2 Stress-strain curves of as grown and prestrained crystals. The stress level indicated on the diagram refers to the resolved shear stress reached during prestraining along [111].

Fig. 3 Low magnification (13×) optical photographs of the gauge length of an as-grown copper crystal deformed in stage I to a shear strain of (a) 1%, (b) 3%, and (c) 5%. Same area is shown in all three photographs.

Fig. 4 Slip-line structures at the same area of an as-grown crystal deformed in stage I to shear strains of (a) 1%, (b) 3%, and (c) 5%.

Fig. 5 Dark-field optical micrographs of the same area of the surface of an as-grown crystal deformed in stage I to a shear strain of (a) 1%, and (b) 5%.

Fig. 6 Active slip lines on the same area after 2% (a) and 4% (b) shear-strain increments in stage II, at a total strain of 7% (as-grown crystal).

Fig. 7 Slip-line structure on the same area of an as-grown crystal deformed in stage II. (a) 5%, (b) 15%.

Fig. 8 Active slip lines formed by a 2% shear-strain increment in stage II, at a total strain of 7% (a), 15% (b) and 23% (c) (as-grown crystal).

Fig. 9 Luders band propagation in the region of small hardening rate of a crystal prestrained by shock loading. Same area of the crystal surface is shown at (a) 0.5%, (b) 0.85%, and (c) 2% shear strains. The left end of the micrographs corresponds to an edge of the crystal.

Fig. 10 Fine structure of the slip bands formed in the region of small hardening rate of a crystal prestrained by shock loading. Same area of the crystal surface is shown at (a) 4.2%, (b) 6.2%, and (c) 12% shear strains.

Fig. 11 Fine structure of the surface of a crystal prestrained by shock loading at the end of the region of small hardening rate (12% shear strain).

Fig. 12 Slip bands formed in the region of linear hardening of a crystal prestrained by shock loading. Same area is shown after (a) 2%, (b) 20% and (c) 30% shear-strain increments.

Fig. 13 Fine structure of the slip bands formed in the region of linear hardening of a crystal prestrained by shock loading. Same area of the crystal surface is shown after (a) 2%, (b) 10%, (c) 20%, and (d) 30% shear-strain increments.

Fig. 14 Active slip lines formed by a 2% shear-strain increment in the region of linear hardening at a total shear strain of (a) 16%, (b) 26%, and (c) 36%, (shock loaded crystal) loading.

Fig. 15 Luders band propagation in the region of small hardening rate of a crystal prestrained to 2.54 kG/mm^2. Same area of the crystal surface is shown at (a) 4.8%, (b) 5.7%, (c) 6.0%, and (d) 9.5% shear strains.

Fig. 16 Fine structure of the slip bands during the Luders band propagation. The crystal was prestrained to 2.54 kG/mm^2.

Fig. 17 Formation of slip bands at the beginning of the region of linear hardening of a crystal prestrained to 2.54 kG/mm^2. (a) and (b) show the same area of the surface with a shear strain increment of 0.1% between them.

Fig. 18 Active slip lines formed by a 2% shear-strain increment in the region of linear hardening, at a total shear strain of (a) 23%, (b) 33%, and (c) 43%. The crystal was prestrained to 2.54 kG/mm^2.

Fig. 19 A plot of the reciprocal length of active slip lines formed by a 2% strain increment in stage II against the total shear strain at which they formed.

Fig. 20 Increase in the distance between pinning points by glide of forest dislocations.

Fig. 21 Formation of a source by cooperative glide of forest dislocations.

Fig. 22 A metastable arrangement of screw dislocations.

Fig. 23 Annihilation of metastable edge dislocations.

Fig. 24 Cross slip at an attractive dislocation intersection.

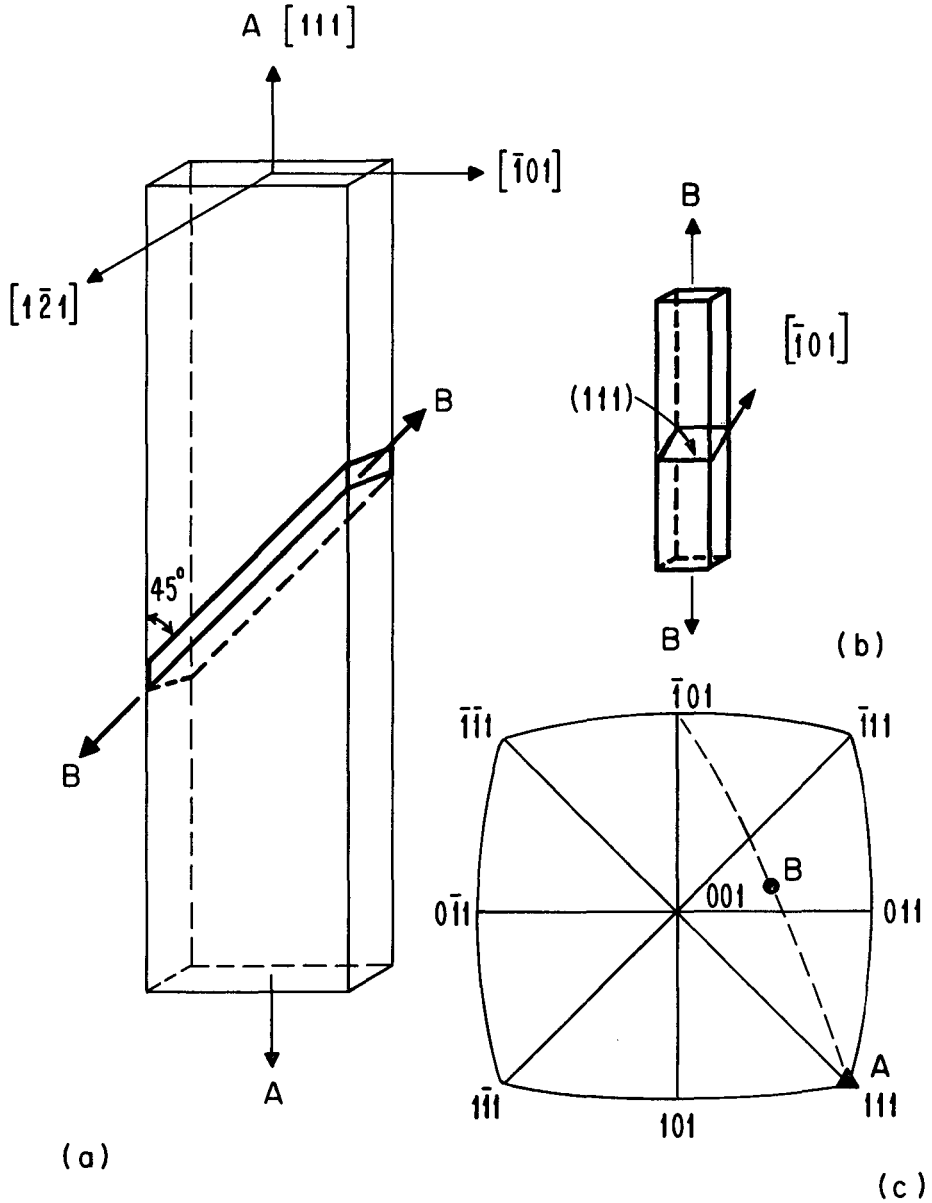

MUB-11515

Fig. 1

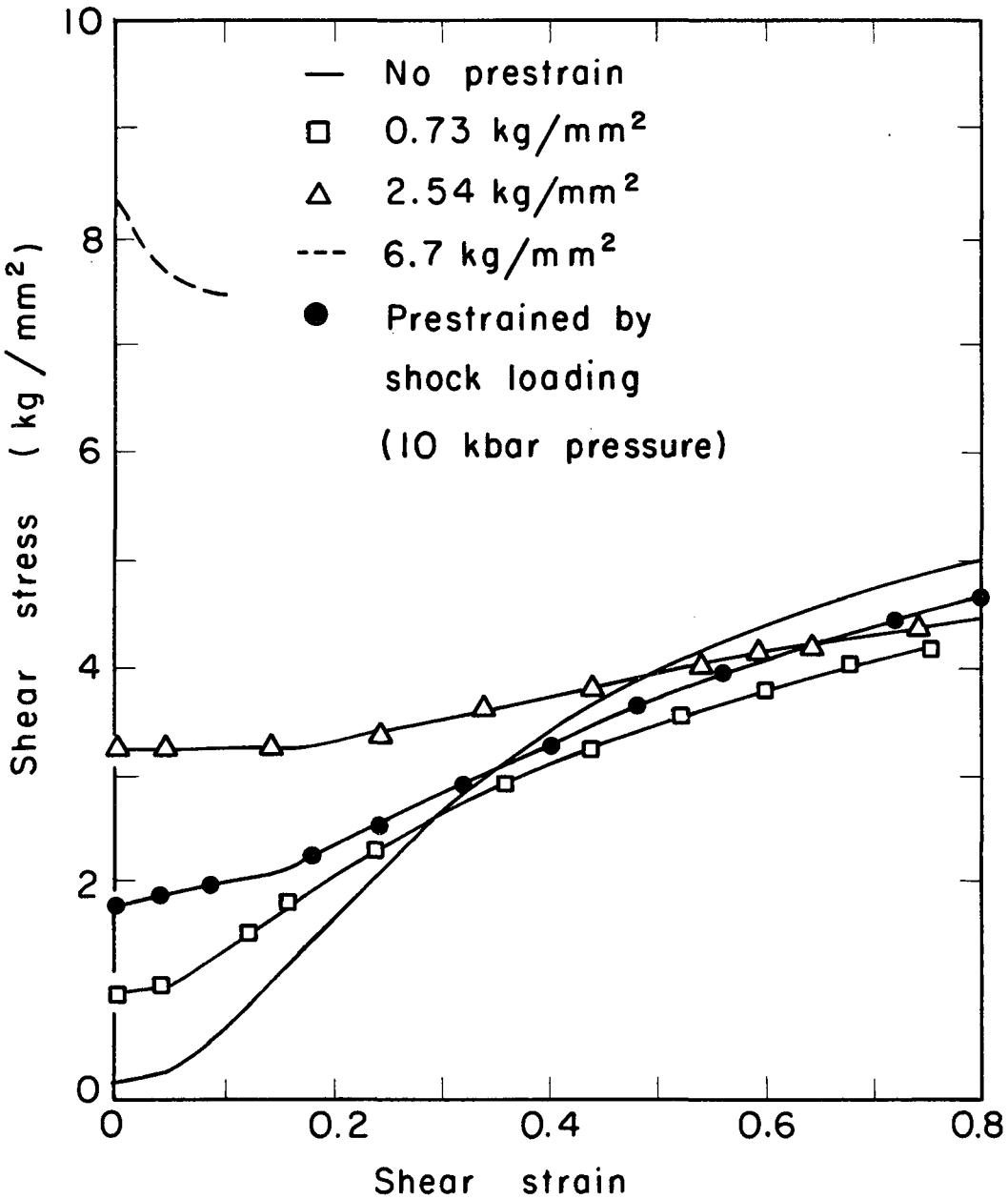

MUB-8771

Fig. 2

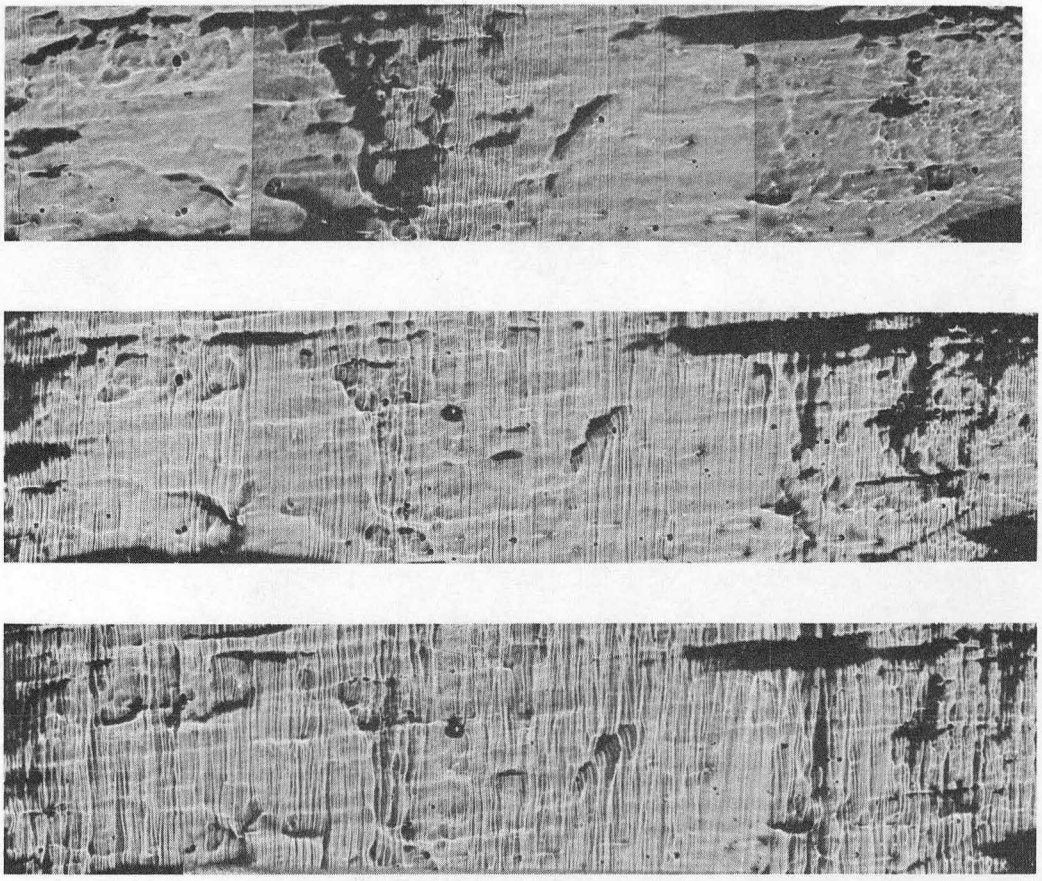

ZN-5958

Fig. 3

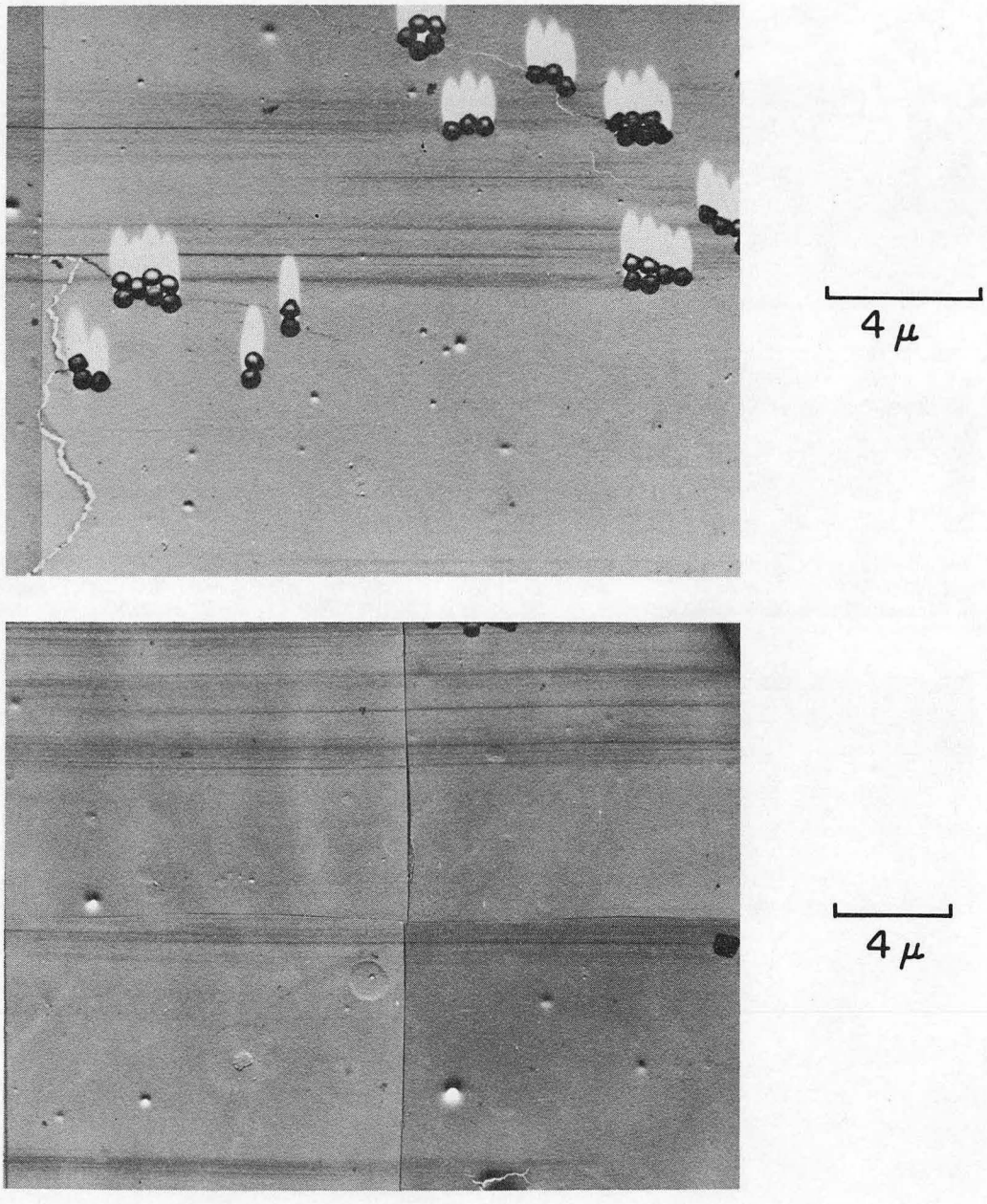

Fig. 4

(a)

(b)

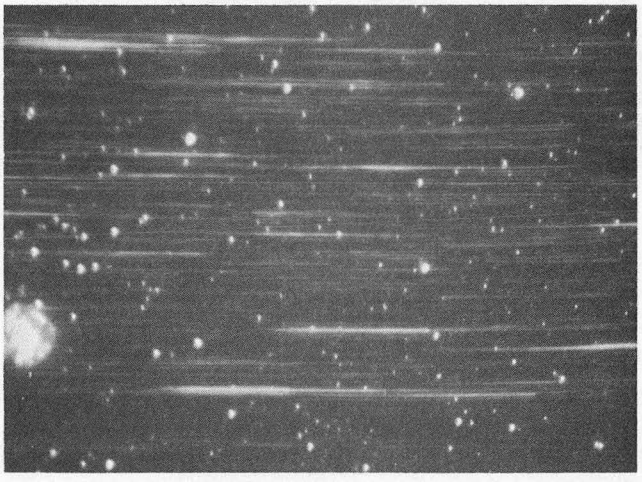

100μ

ZN-5678

Fig. 5

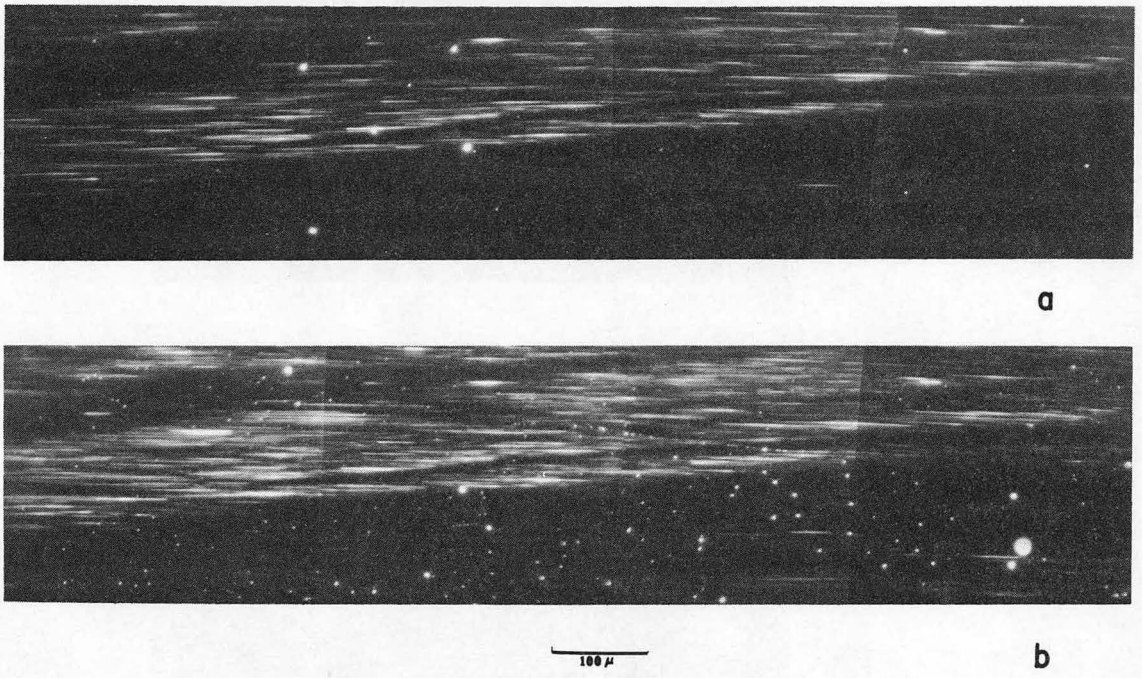

Fig. 6

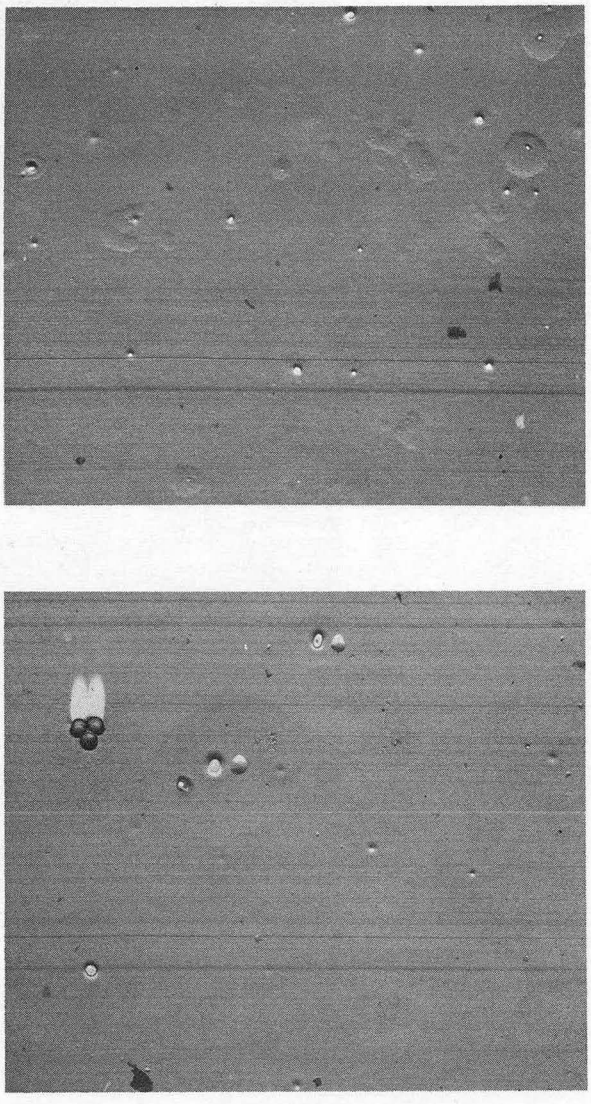

Fig. 7

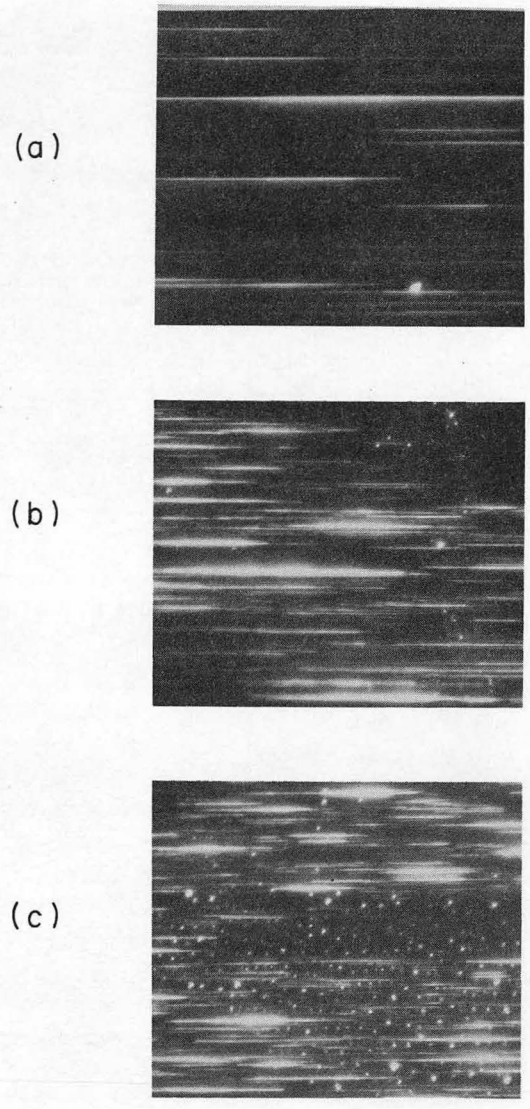

Fig. 8

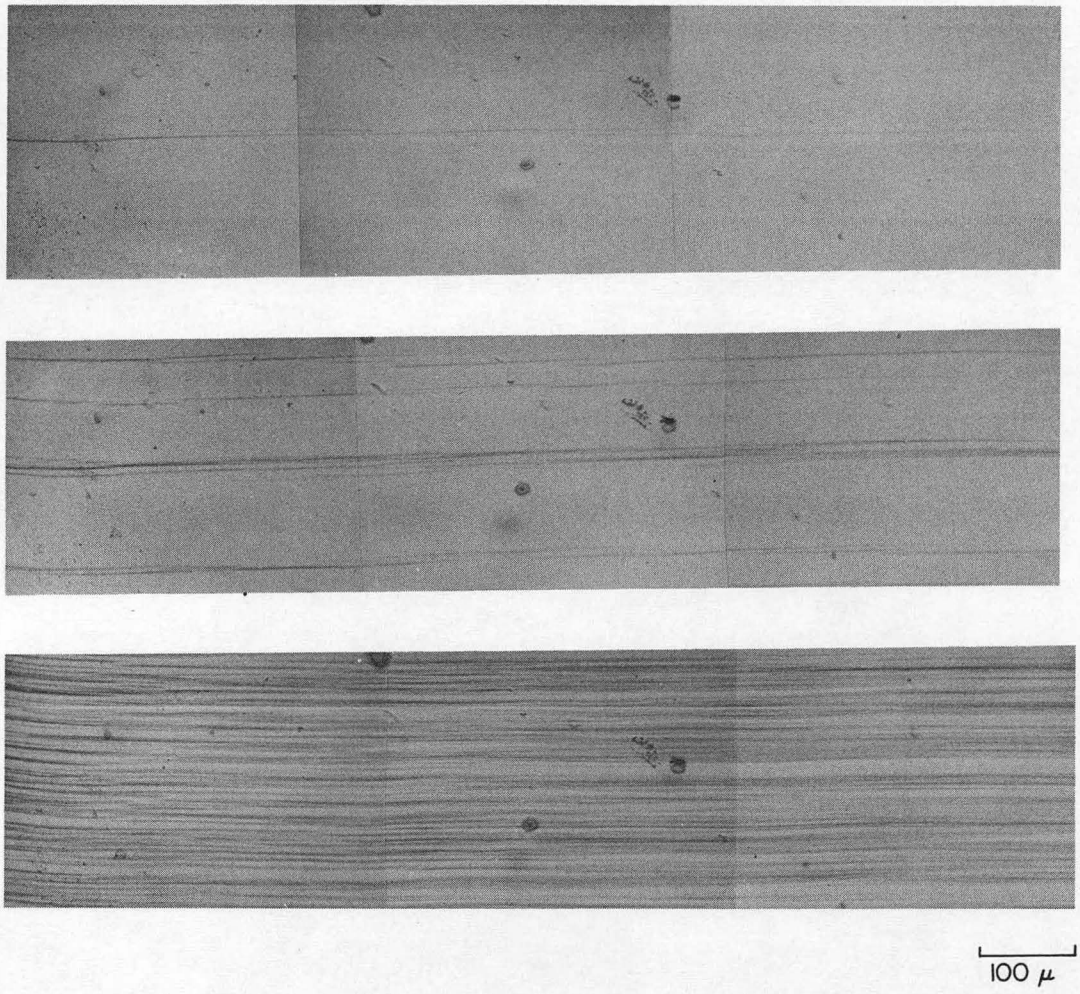

Fig. 9

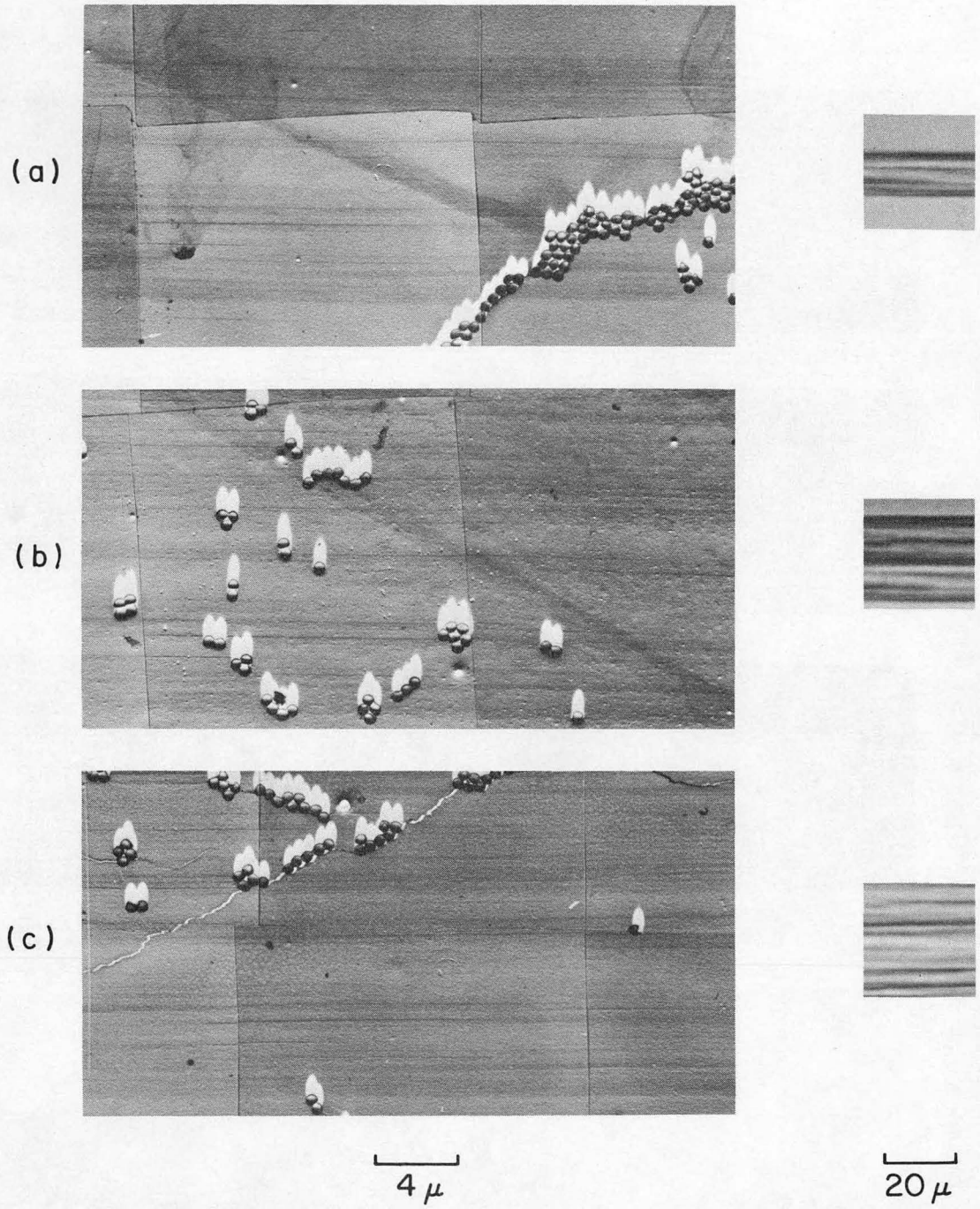

Fig. 10

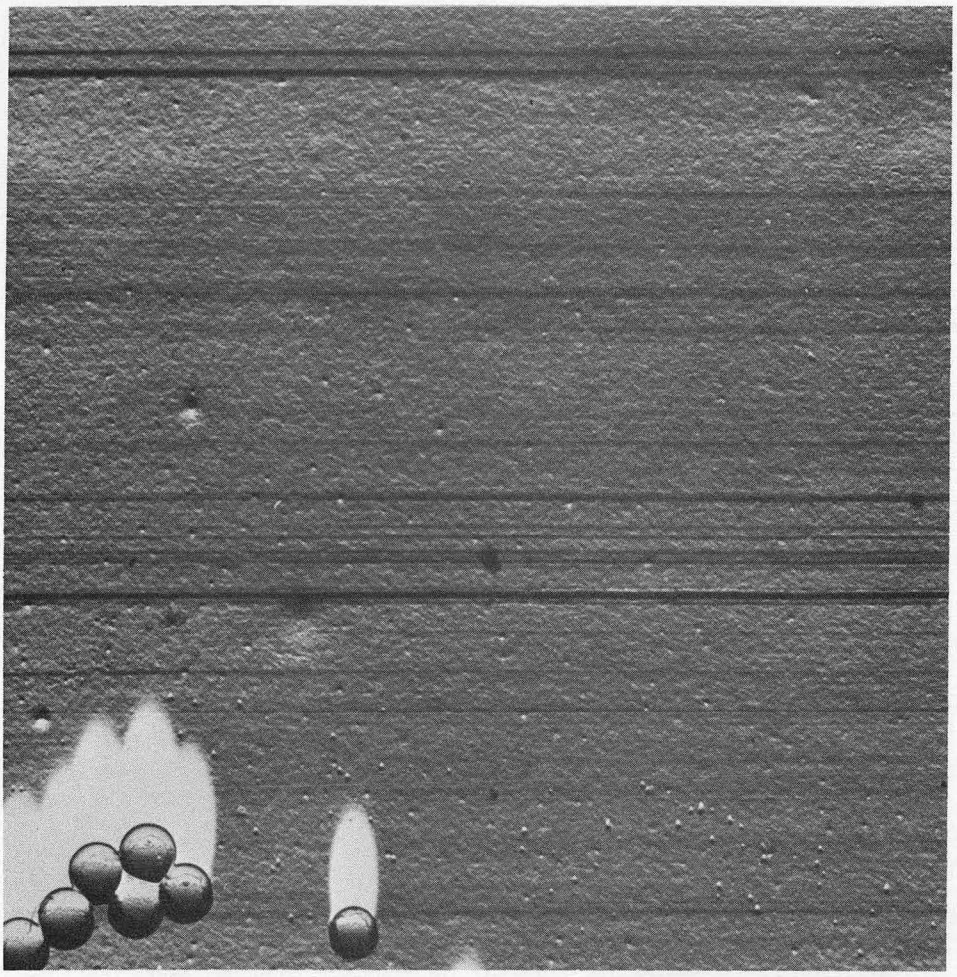

1 μ

ZN-5675

Fig. 11

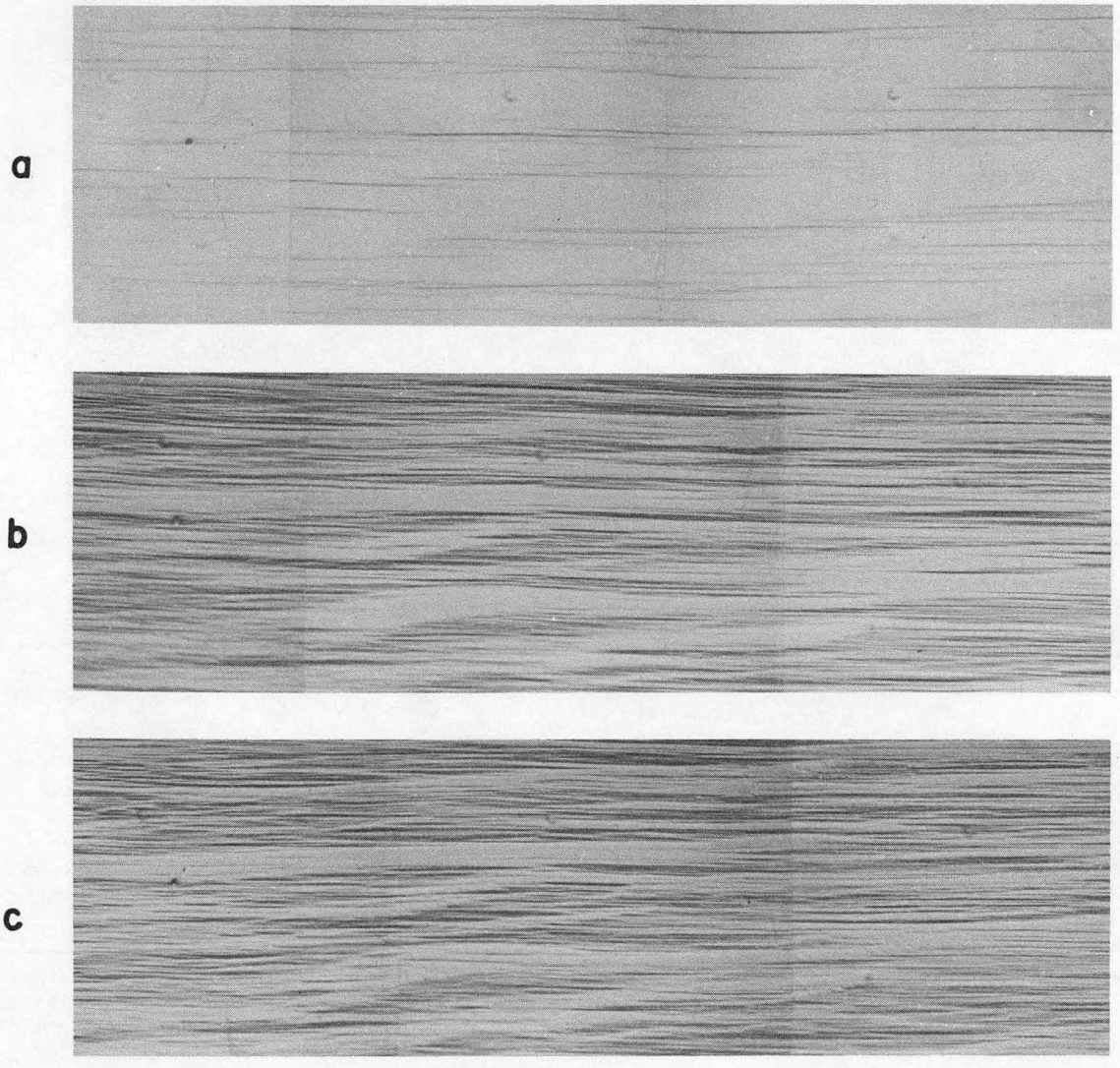

ZN-5969

Fig. 12

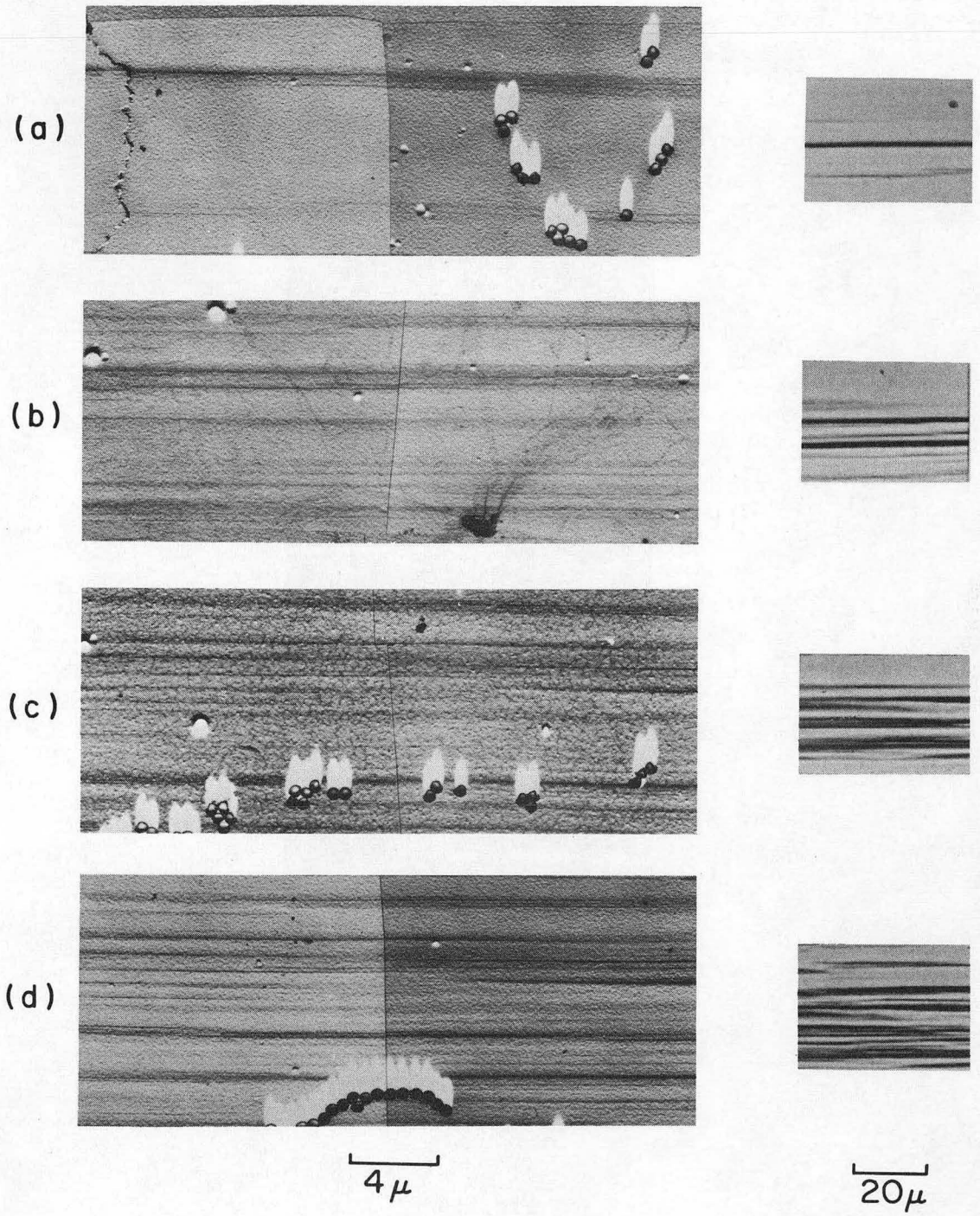

Fig. 13

Fig. 14

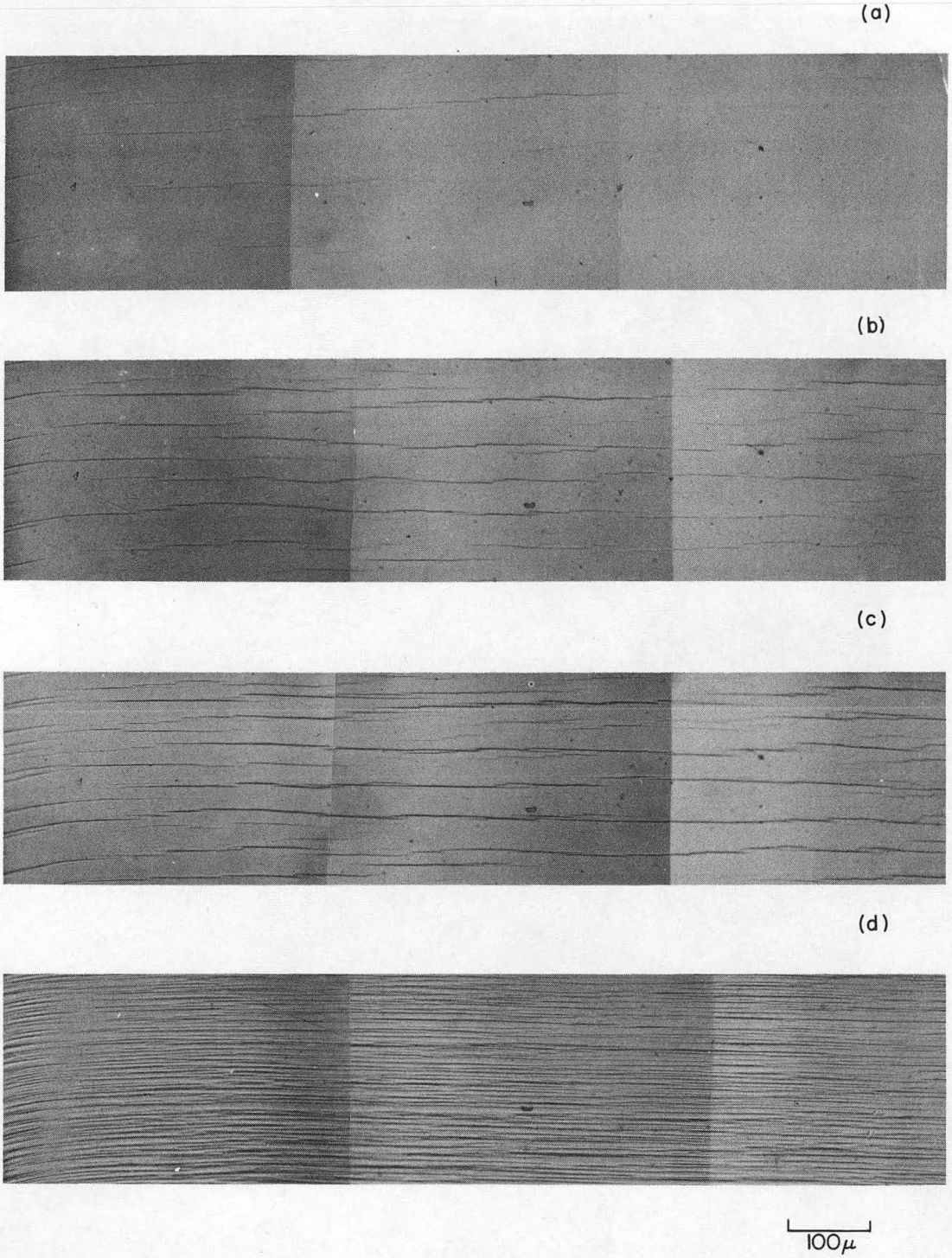

Fig. 15

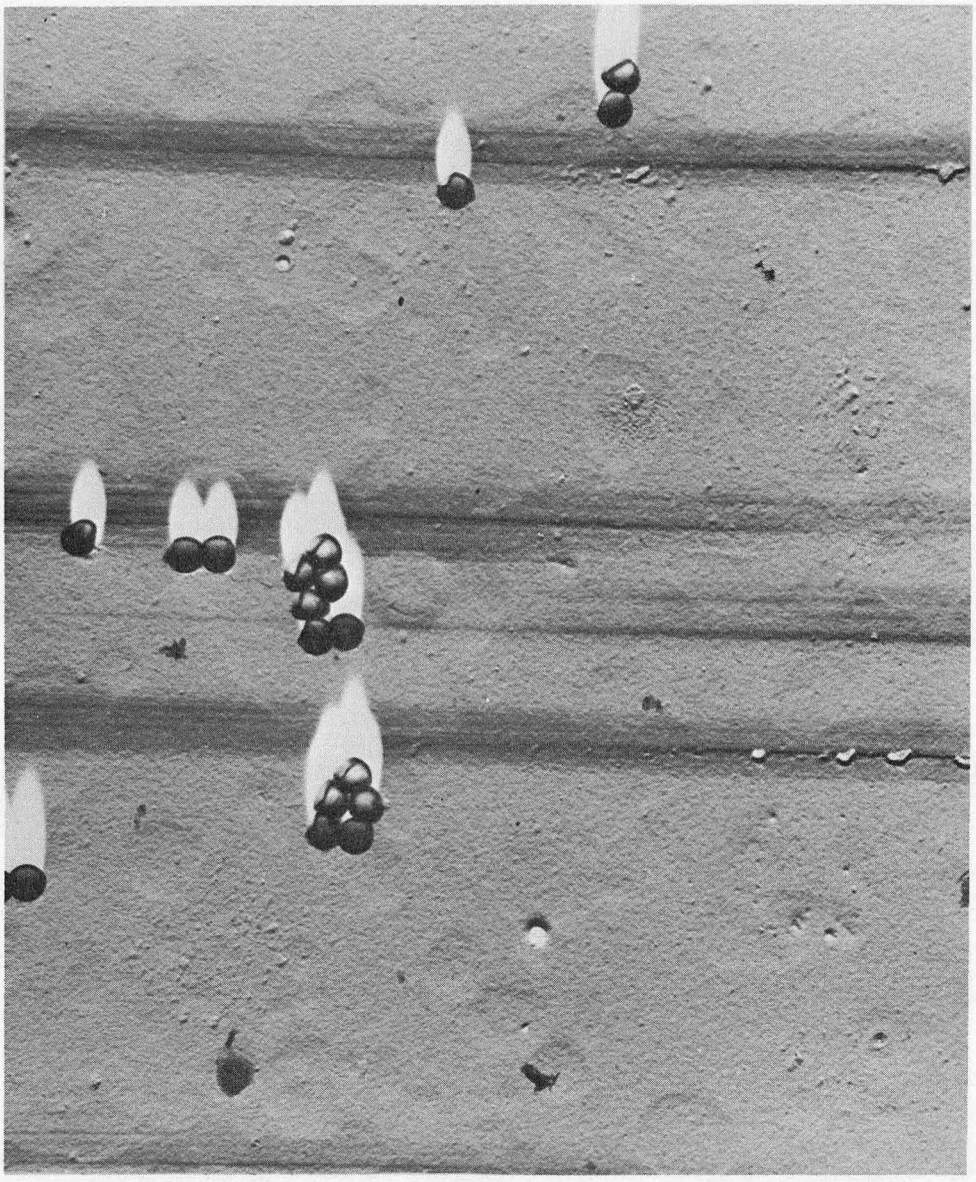

2 μ

ZN-5690

Fig. 16

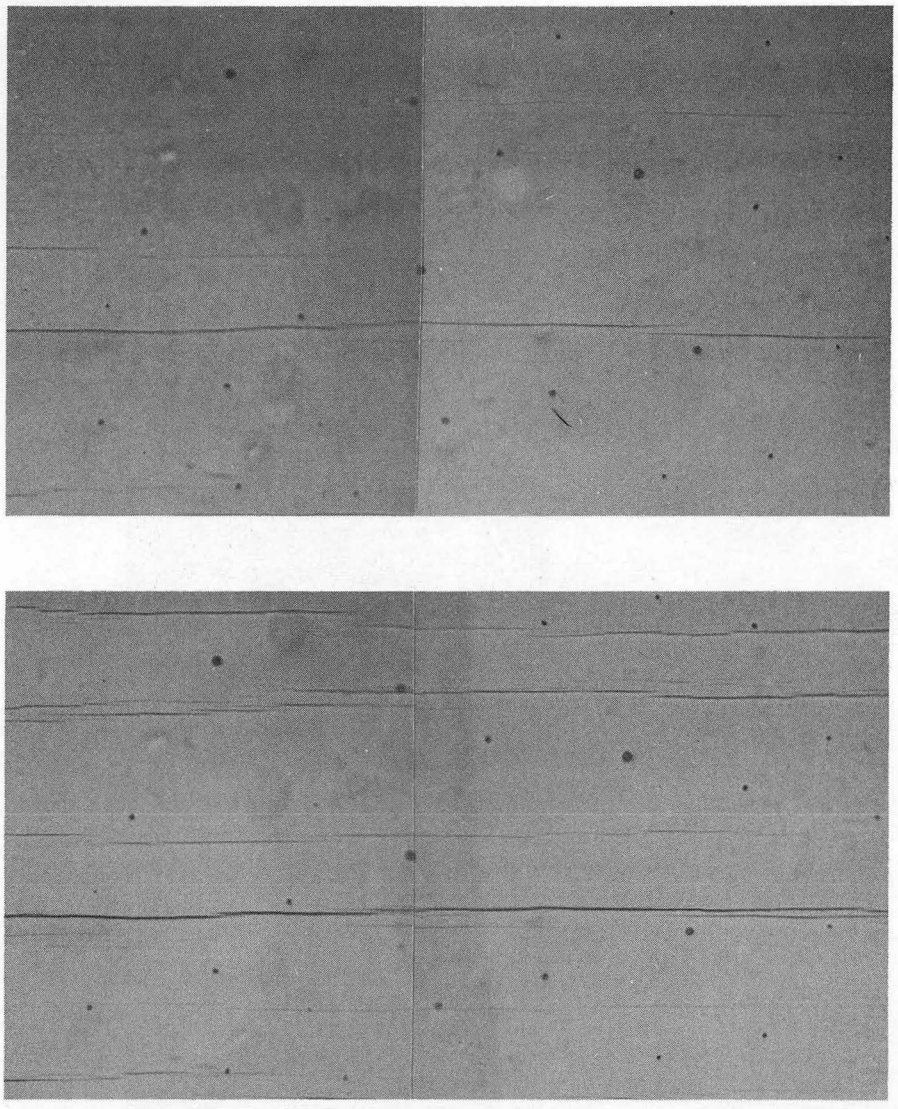

Fig. 17

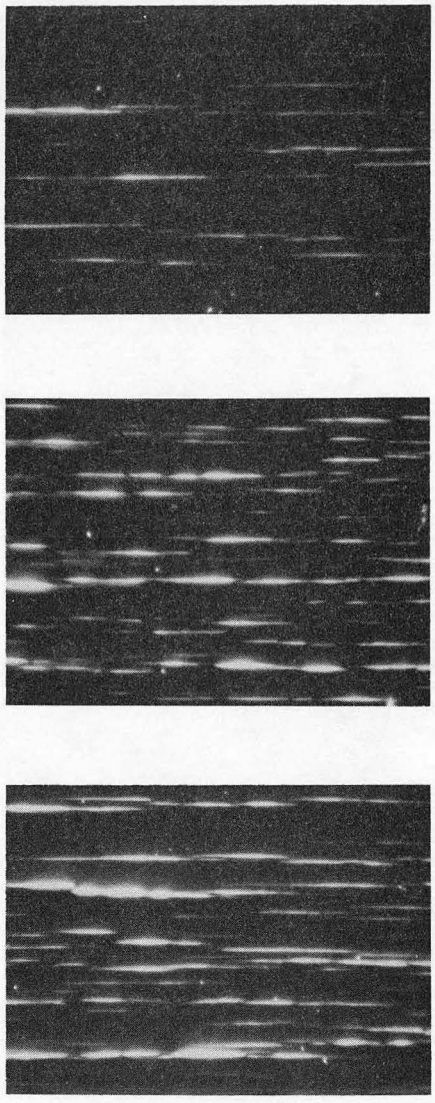

Fig. 18

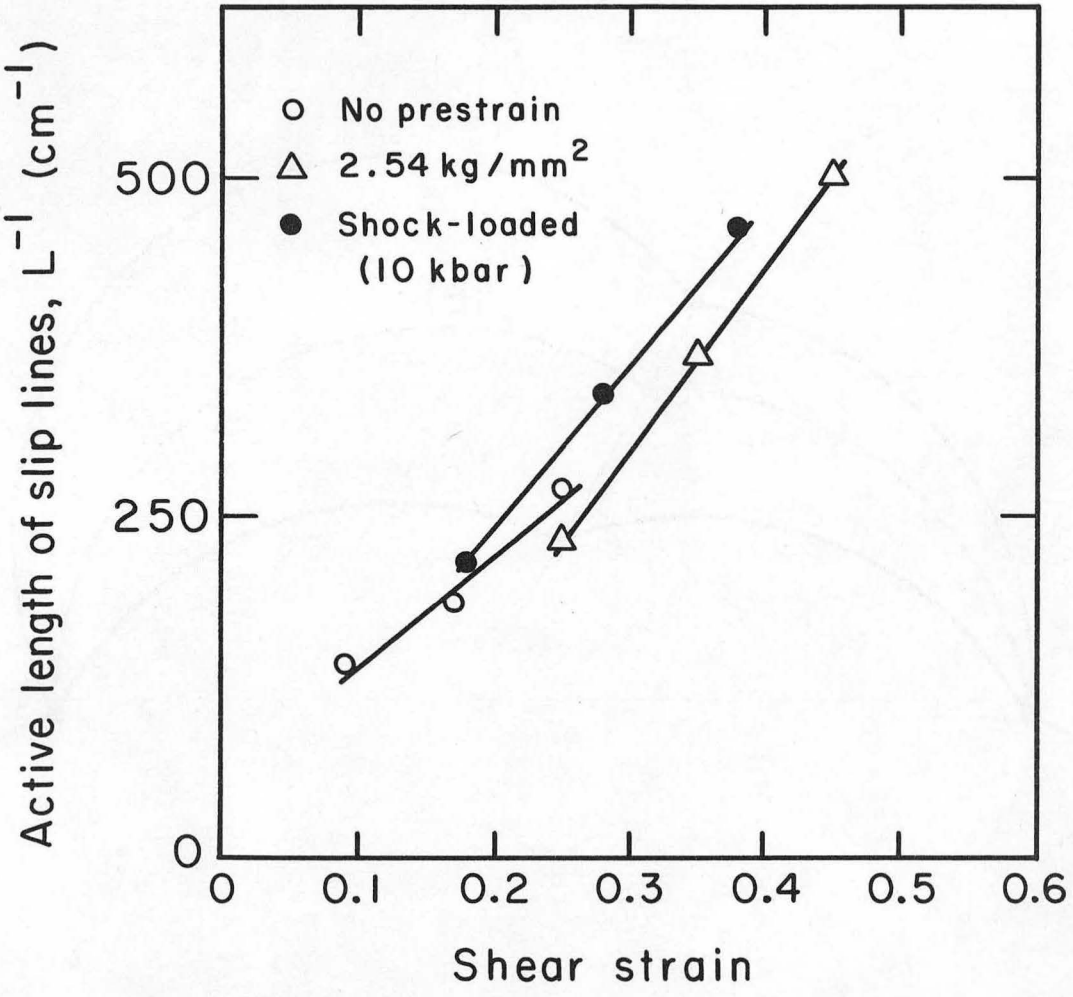
No prestrain
2.54 kg/mm²
Shock-loaded
(10 kbar)
Active length of slip lines, L⁻¹ (cm⁻¹)
500
250
0
0
0.1
0.2
0.3
0.4
0.5
0.6
Shear strain
MUB-11513

Fig. 19

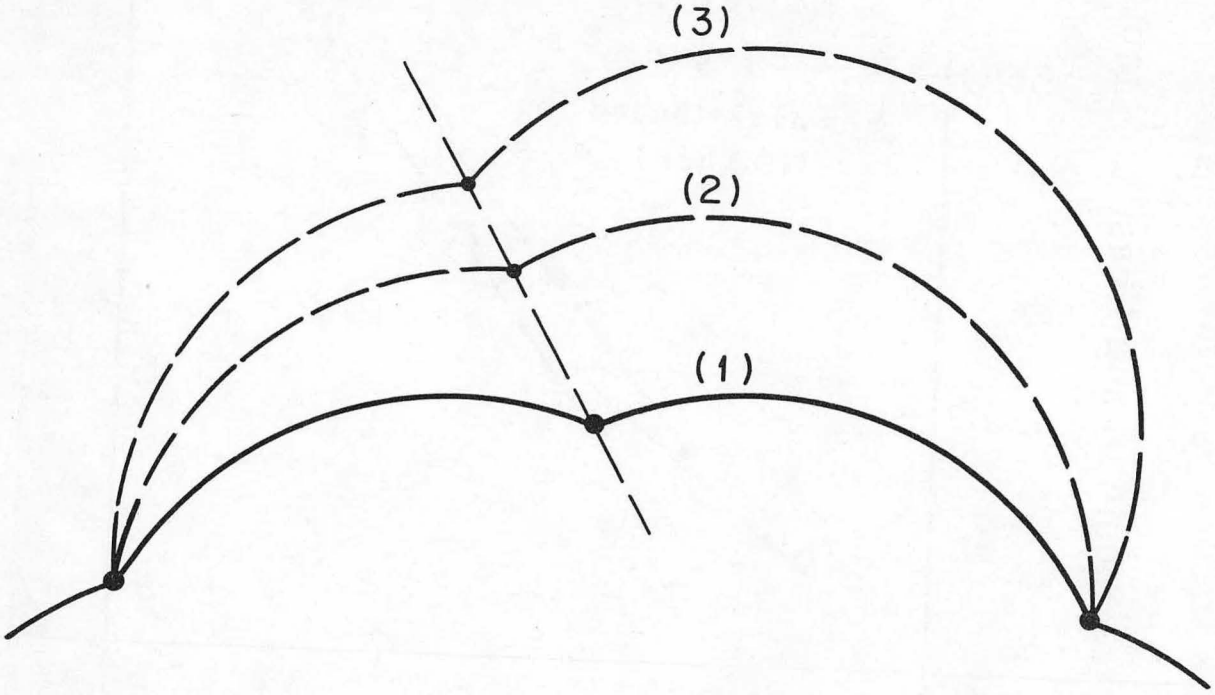

MUB-9303

Fig. 20

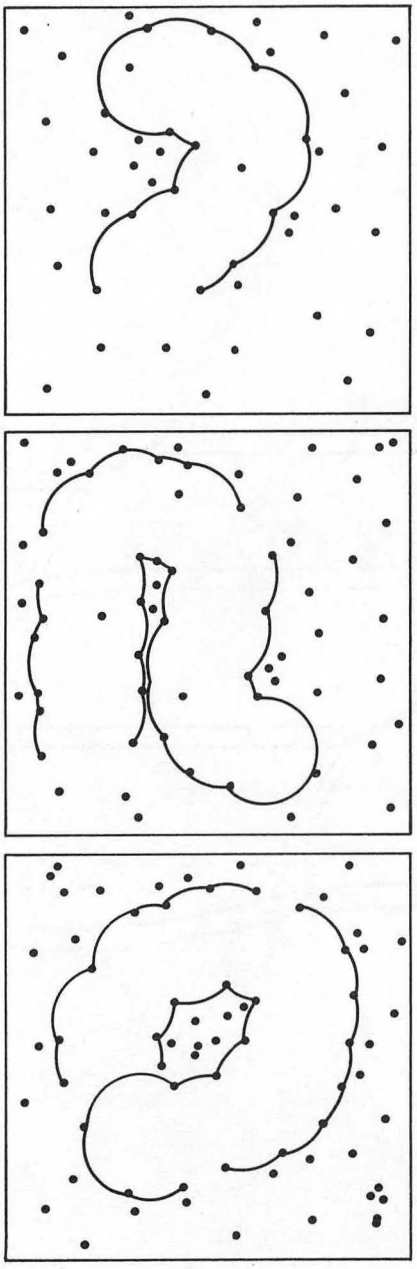

MUB-9304

Fig. 21

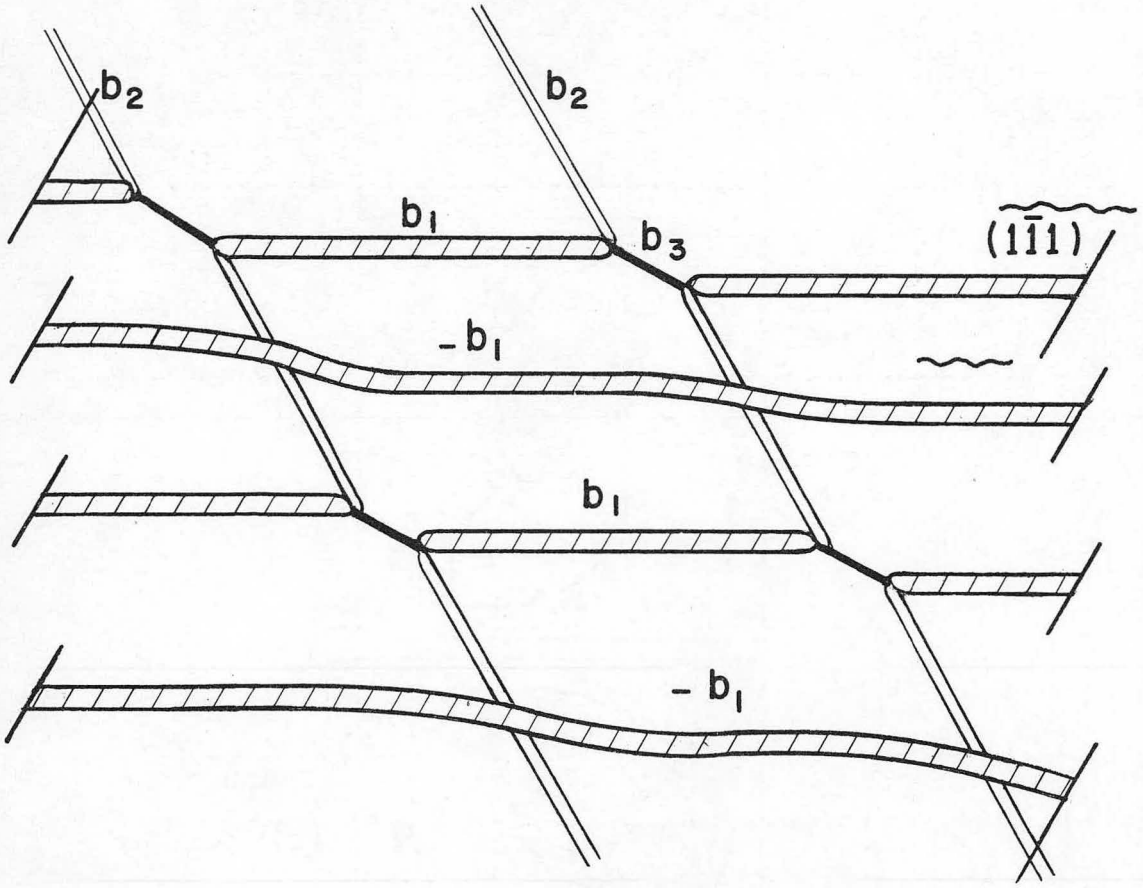

MUB-8772

Fig. 22

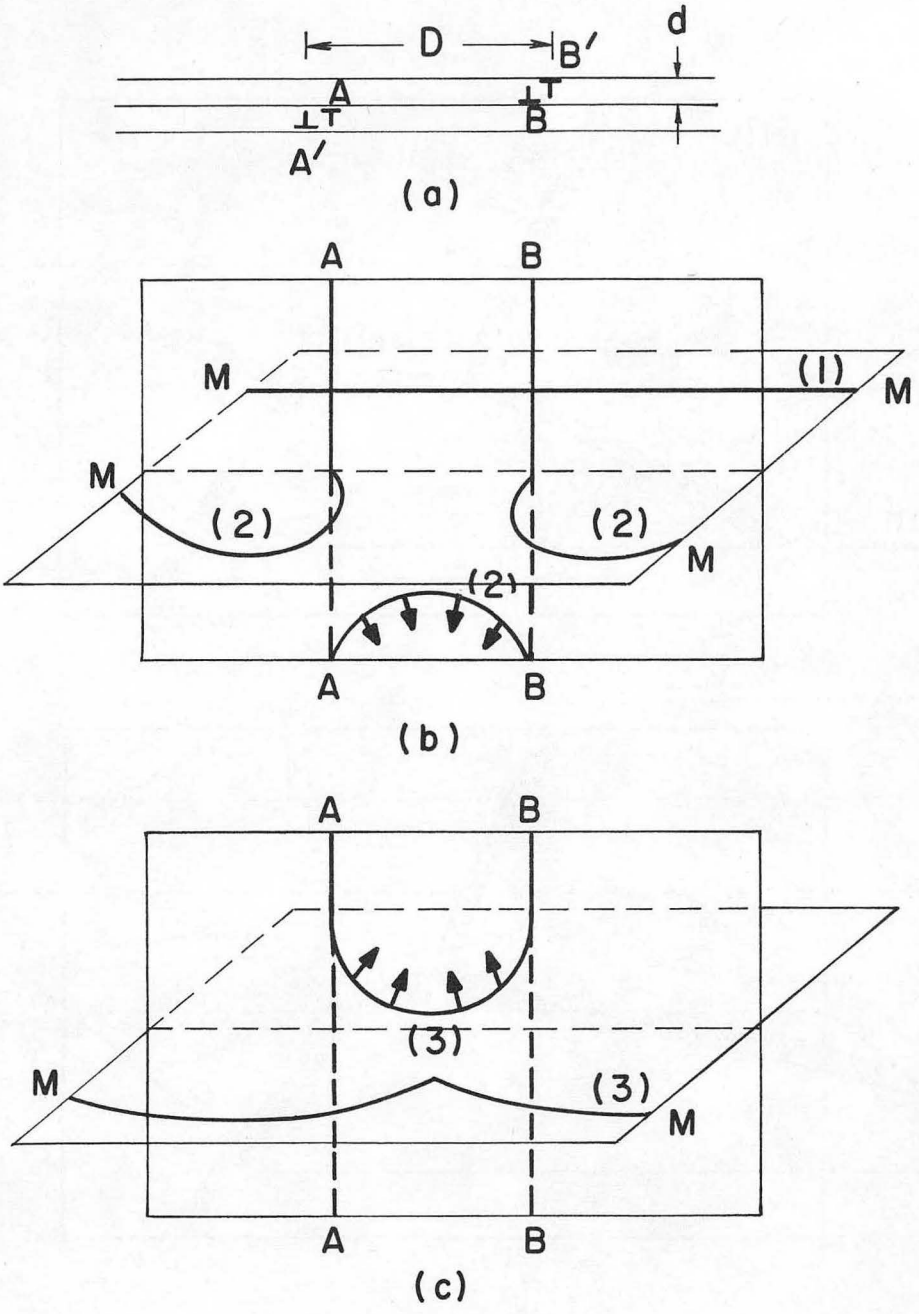

MUB-8770

Fig. 23

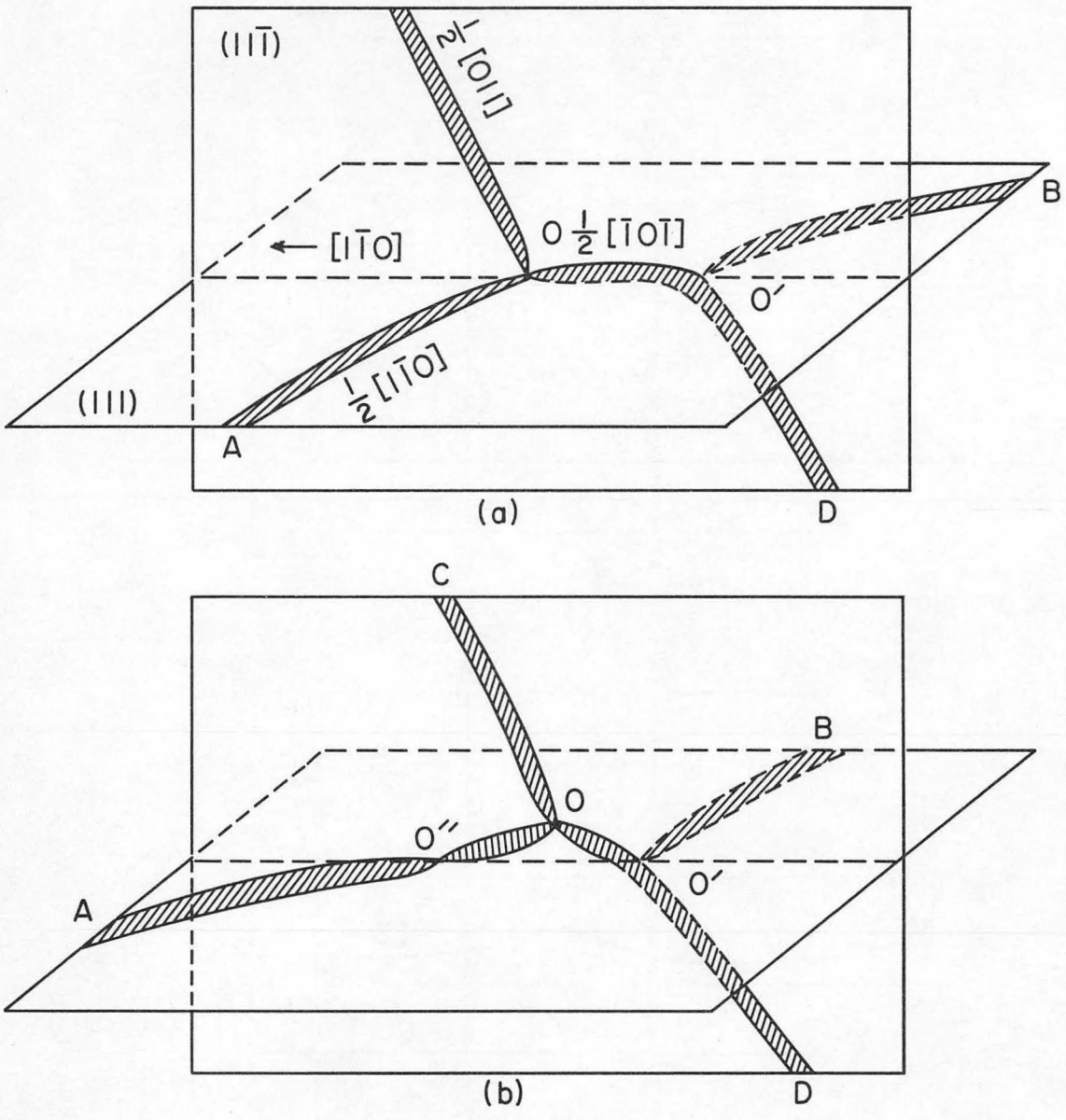

MU B-13145

Fig. 24